Supporting Information

Experimental Section

Reagents and equipments. All DNA sequences were all synthesized by Sangon (Shanghai, China). The sequences are as follows:

DNA-1(AG_3): 5′- NH_2-$(CH_2)_6$-AGGGTTAGGGTTAGGGTTAGGG-$(CH_2)_6$-SH-3′

DNA-2 (C-rich DNA): 5′-CCCTAACCCTAACCCTAACCCT-3′

DNA-3 (Control): 5′-dA_{22}-3′

Tris-(2-carbozyethyl) phosphine hydrochloride (TCEP) was purchased from Sigma-Aldrich (St. Louis, MO) and used without further purification. 6-Mercaptohexanol (MCH) was purchased from Fluka and used as received. Ferrocenecarboxylic acid (Fc), 1-ethyl-3-(3-dimethyl-aminopropyl) carbodiimide hydrochloride (EDC), and N-hydroxysulfosuccinimide (Sulfo-NHS) were purchased from Sigma-Aldrich. All aqueous solutions were prepared using ultra-pure water (18.2 MΩ, Milli-Q, Millipore).

The metallo-supramolecular cylinder $[Ni_2L_3]Cl_4$ was synthesized and purified as previously reported. The enantiomerically pure $[Ni_2L_3]Cl_4$ was obtained by using a cellulose (~20 μm, Aldrich) column and eluting with 20mM NaCl aqueous solution. The purity is more than 95%, which was determined by ESI-MS and elemental analysis. UV-vis spectroscopy was used to determine the enantiomer concentration. The samples of purified M- and P-enantiomer were collected and freeze-dried for future use.[1,2]

Labeling of Fc to NH_2-Modified Oligonucleotides. The ferrocene (Fc) label was conjugated to the 5′-NH_2-moiety of the oligonucleotide (DNA-1), using the succinimide coupling (EDC-NHS) method. Briefly, 100 μL of 10μmol DNA-1 was mixed with 100 μL of 10mM PBS (pH 7.4) containing 10mmol of ferrocenecarboxylic acid (FcA), 50mM EDC, 25mM Sulfo-NHS, followed by incubation for 2h at 37℃. The excessive ferrocenecarboxylic acid was subsequently dialyzed against 10 mM PBS buffer through the molecularporous memebrane tubing (MWCO: 2000, Spectrum Laboratories, Inc. US). The resulting DNA solution was stored at 4℃ for use.

Electrode Cleaning and E-DNA Sensor Preparation. The oligo 1 modified sensor was fabricated by using gold disk electrodes (Φ = 2 mm, CH Instruments, Austin, TX). The electrodes were prepared by polishing with 0.3 and 0.05 μm deagglomerated γ alumina (BUEHLER, UAS) suspensions followed by sonication in water and multiple steps of electrochemical cleaning before modification with the thiolated Fc-tagged probe DNA. The clean gold surface was incubated with a 0.1 μM solution of thiolated Fc-labeled DNA oligomer pretreated with TCEP in buffer (10 mM Tris buffer, 1.5M LiCl, 10m M $MgCl_2$, pH 7.2) for 12 h at room temperature. The surface was then rinsed with buffer and subsequently passivated with 6-mercaptohexanol in the Tris buffer for 1 h. Then, the electrodes were rinsed again with buffer (10 mM Tris buffer, 10m M LiCl, pH 7.2) and stored in the Tris buffer prior to measurements.

Electrochemical Measurements. Alternating current voltammetry (ACV) were performed with a CHI 660B electrostation in a standard cell with a platinum counter electrode and an Ag/AgCl reference electrode. The E-DNA sensor measurements were conducted by monitoring the modified working electrode in Tris buffer (10 mM Tris salt, 10 mM LiCl, pH 7.2) using ACV with a step potential of 10 mV, amplitude of 25 mV, and a frequency of 100 Hz. Electrochemical impedance spectroscopy (EIS) was performed using Solartron Instrument equipped with S11287 electrochemical interface and S11255 HF Frequency response analyzer in 10m M Tris buffer (10m M LiCl, p H= 7.2) as the supporting electrolyte. The impedance spectra were recorded at potential of 0.165V within the frequency range of 10^{-2}-10^{5} Hz. The amplitude of the applied sine wave potential in each case was 5 mV.

For all G-quadruplex ligands detection measurements, ligands were diluted with the aqueous Tris buffer, and then the modified electrodes were incubated in each sample containing different concentrations of ligands for 20min at room temperature except the time-course study. Prior to measurement, washing with the measured buffer is necessary. For the target hybridization measurements, the electrodes were incubated in 1 μM complementary G-quadruplex DNA or 1 μM dA_{22} oligomer solution for 1 h, and the regeneration was done with a simple 30s ultrapure water rinse. The experimental temperature was controlled at 15℃.

To measure the apparent electron transfer rates, we performed square wave voltammetry (SWV) after 20min of target binding. SWV measurement were conducted over a potential range of 0.7 to –0.2V, using a 4mV step potential and

25mV amplitude at frequencies ranging from 1 to 100Hz. At each SWV mearsurement frequency, we calculated the ratio between the Fc peak current and the frequency. This peak current-to-frequency ratio was normalized and plotted against the SWV measurement frequency. The apparent electron transfer rate was estimated from the critical frequency, which was defined as the normalized peak current maximum.[3,4]

UV Melting and Circular Dichroism Measurements. UV melting studies were carried out on JASCO V-550 UV-vis spectrophotometer, equipped with a Peltier temperature control accessory. CD spectra were measured on JASCO J-810 spectropolarimeter. The optical chamber of the CD spectrometer was deoxygenated with dry purified nitrogen (99.99%) for 45 min before use and kept the nitrogen atmosphere during experiments. Three scans were accumulated and automatically averaged.

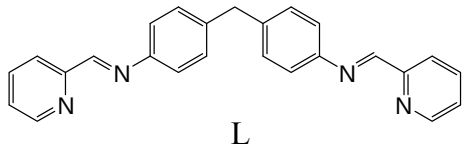

L

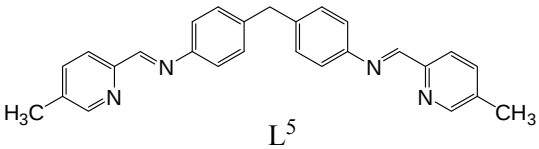

L^5

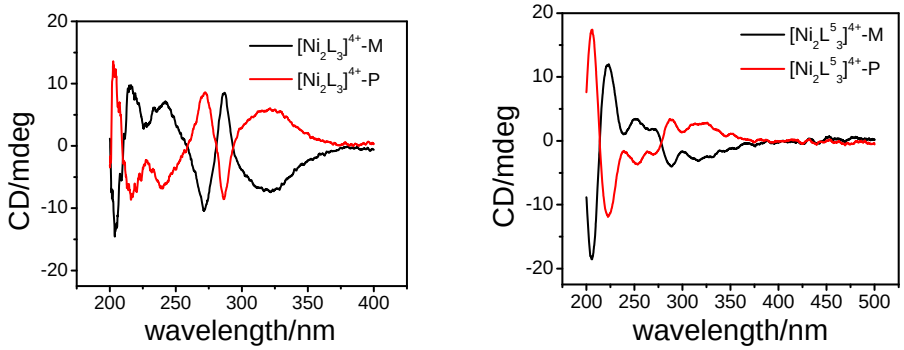

Supplementary Figure S1. The structure of bis(pyridylimine) ligand L and L^5 with alkyl substituent.CD spectra of the M-enantiomer (black) and P-enantiomer (red) of $[Ni_2L_3]^{4+}$(left) and $[Ni_2L^5{}_3]^{4+}$(right).

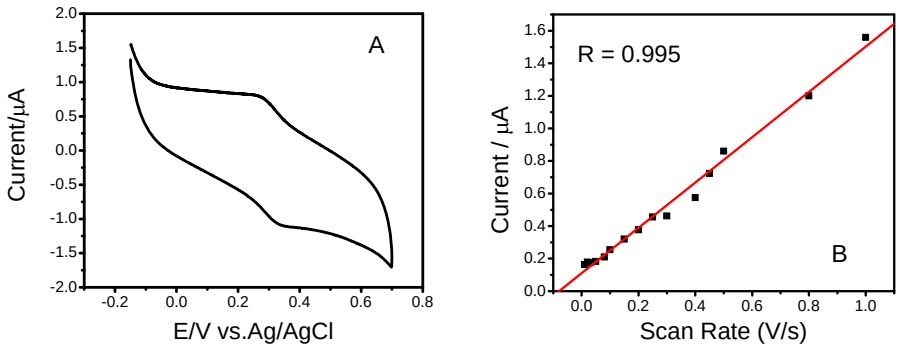

Supplementary Figure S2. (A) A cyclic voltammogram of Fc-AG_3-coated Au electrode in 10mM Tris buffer solution (10mM Li^+, pH=7.2). Scan rate: 100mV/s. (B) The linear relationship between peak currents and scan rates confirms that the redox species is confined to the electrode surface.

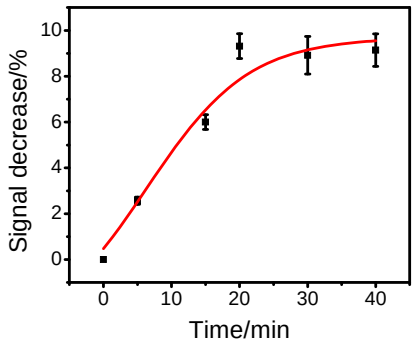

Supplementary Figure S3. Incubation time dependence. The signal response was measured after incubation in 0.15μM $[Ni_2L_3]^{4+}$-P solution with different time. P-cylinder facilitated the formation of intramolecular G-quadruplex structures within several minutes , and the signal decrease 9.6% after 20 minutes.

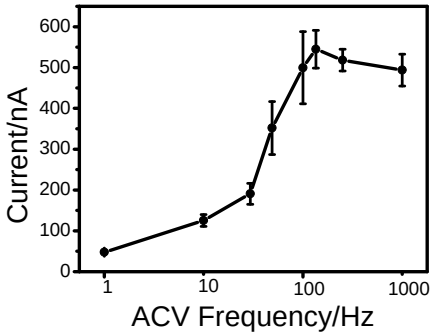

Supplementary Figure S4. ACV frequency optimization. Sensor peak currents were measured using standard parameters at frequencies from 1Hz to 1000Hz. The frequency is displayed in a logarithmic scale, and a plateau of 100Hz was chosen.

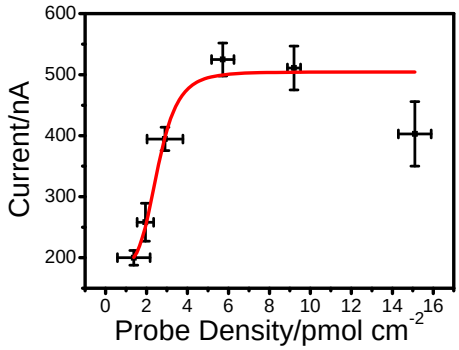

Supplementary Figure S5. Optimization of the probe surface density of E-DNA sensor. The probe surface density is controlled by adjusting the probe concentration (0.01, 0.02, 0.05,0.1, 0.5, 1μM) employed during sensor fabrication and subsequently determined using a previously established relationship with ACV peak current [4] described in Eq. 1:

$$I_{avg}(E_0)=2nfFN_{tot}[\sinh(nFE_{ac}/RT)]/[\cosh(nFE_{ac}/RT)+1] \quad [1]$$

In which $I_{avg}(E_0)$ is the average peak current in the AC voltammograms, n is the number of electron transferred per redox event (with Fc label n=1), *f* is the frequency of the applied ACV perturbation, F is the Faraday constant, N_{tot} is the number of

electroactive DNA probe in moles, E_{ac} is the peak amplitude (E_{ac} =25 mV in experiment), R is the universal gas constant, and T is the temperature (T=288.15K). The apparent electrode area-measured from the gold oxide reduction peak area during gold working electrode cleaning in 0.05M H_2SO_4 solution-was used to calculate the probe surface density from N_{tot}. The optimal modified probe concentration was 0.1 μM with a calculated surface density of 5.72 pmol/cm^2.

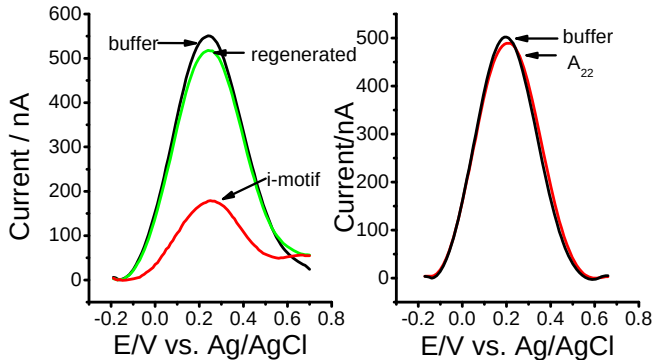

Supplementary Figure S6. Alternating current (AC) voltammograms of the E-DNA sensor in the present of the complementary C-rich DNA (1μM, left) and control strand dA_{22} DNA (1μM, right).

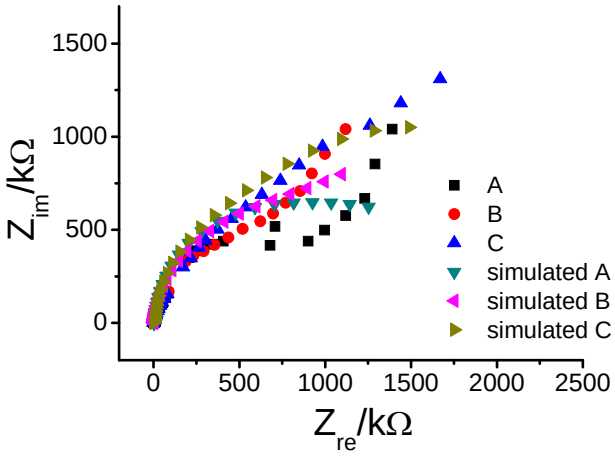

Equivalent electronic circuit:

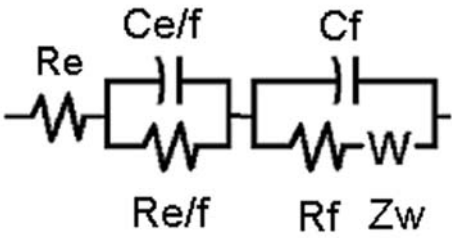

Supplementary Figure S7. Nyquist plots in 10m M Tris buffer at 0.165V for (A) and (simulated A): Fc-AG_3-modified Au electrode, (B) and (simulated B): Fc-AG_3/MCH-modified Au electrode, (C) and (simulated C): After exposure of (B) into 5μM $[Ni_2L_3]^{4+}$-P solution. Frequency range: 10^{-2}-10^{5}Hz; AC amplitude: 5m V. The equivalent electronic circuit was shown below. The ZSimpWin TM electrochemical impedance analysis software was used to deal with the EIS results.

Table S1. EIS results obtained by fitting of experimental data to inset circuit of Figure S7. Each EIS data has been measured for four times.

	R_e, Ωcm^2	$C_{e/f}$, $\mu F\ cm^{-2}$	$R_{e/f}$, Ωcm^2	C_f, $\mu F\ cm^{-2}$	R_f, $k\Omega cm^2$	$Zw\times10^{-5}$
A	1822±36.5	3.54±0.19	220.1±63.6	35.34±6.92	113.2±29.8	0.3437±0.11
B	1978±112.4	4.27±0.33	380.2±139.1	51.9±15.2	151.5±32.7	0.3366±0.06
C	1895±62	1.86±0.04	2994±383.2	24.72±8.6	316.8±45.3	0.4982±0.18

The impedance data were analyzed on the basis of the Vorotyntsev theoretical model of a surface-confined redox system that takes into account the charge-transfer process at the film/electrolyte interface as well as charge diffusion through the film.[5] No significant difference was found in the solution resistance, R_e. The combining $[Ni_2L_3]^{4+}$-P cause the redox label away from the electrode surface, leading to significant increase in the electron-transfer resistance as the electeolyte/film interface $R_{e/f}$, in accord with the decreased signal of ACV. It also resulted in an increase in the interpolate spacing between the electrode surface and the redox active center, reflected as a decrease in $C_{e/f}$ (used as an constant phase element, CPE, to improve the fitting of the experimental data). At the same time, the film thickness increased must give a decreased film capacitance, C_f. R_f would be the resistance of the film, which increased slightly. The Warburg impedance Zw, was resulting from diffusion of the redox probe.

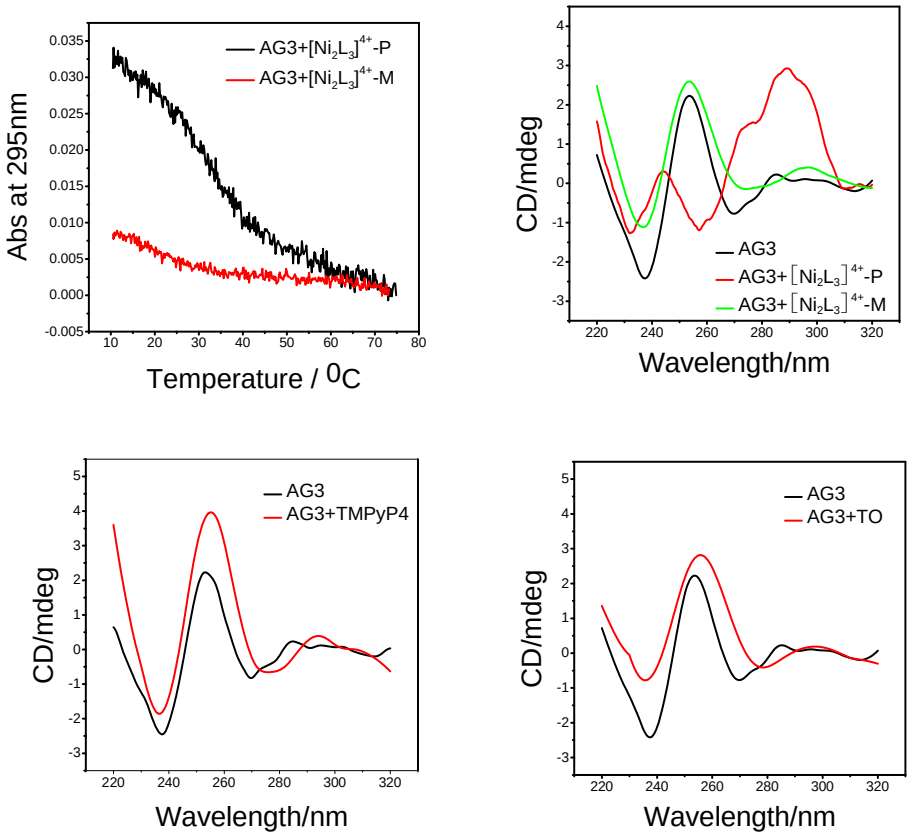

Supplementary Figure S8. UV melting and CD spectra of AG_3 solution containing $[Ni_2L_3]^{4+}$-P, $[Ni_2L_3]^{4+}$-M, TMPyP4 and TO.

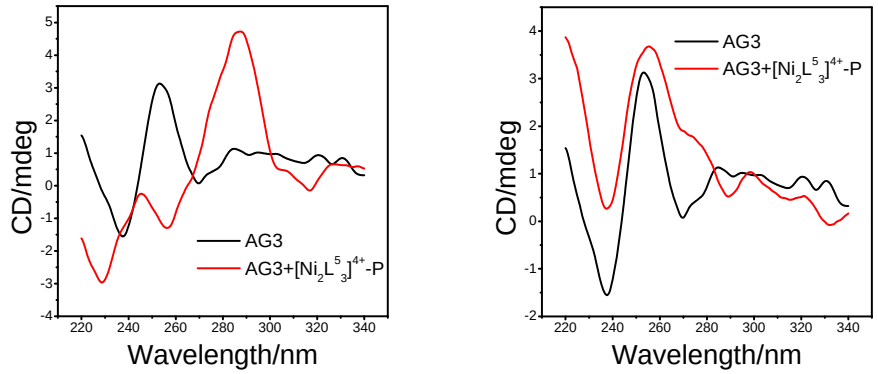

Supplementary Figure S9. CD spectra of AG_3 solution containing $[Ni_2L^5{}_3]^{4+}$-P and $[Ni_2L^5{}_3]^{4+}$-M.

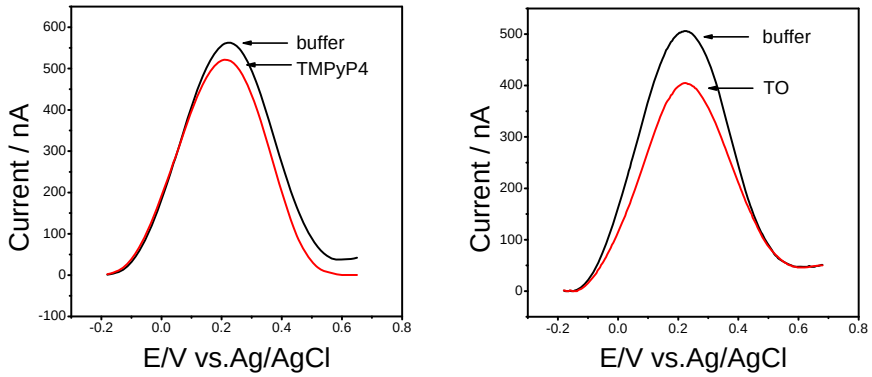

Supplementary Figure S10. Alternating current (AC) voltammograms of the E-DNA sensor after incubation with 5μM TMPyP4 (left) and TO (right) solutions.

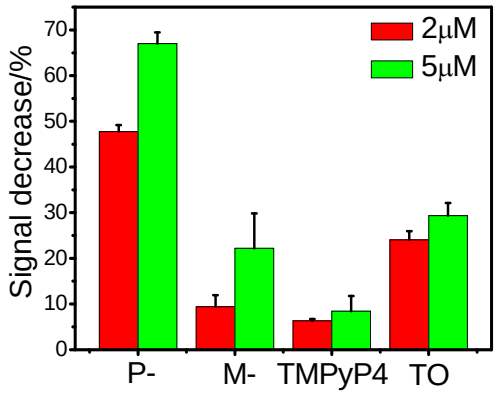

Supplementary Figure S11. E-DNA sensor can readily discriminate between $[Ni_2L_3]^{4+}$-P, $[Ni_2L_3]^{4+}$-M, TMPyP4, and TO at the same concentration of 2μM and 5μM. At the same concentration of 5 μM, the signal decrease was about 71% for P-enantiomer and only 22.2 % for M-enantiomer, with the value of $(I_0\text{-}I_{NiP})/(I_0\text{-}I_{NiM})$ only about 3.2. The enantioselective recognition ratio would be as high as 5 at the concentration of 2 μM. Such a large difference in electrochemical signal change made this E-DNA sensor practically useful for the enantioselective recognition of the metallo-supramolecular complex. Furthermore, both of the TMPyP4 and TO signal decreases were much smaller than $[Ni_2L_3]^{4+}$-P, comparable with $[Ni_2L_3]^{4+}$-M solution.

References:

[1] H. J. Yu, X. H. Wang, M.L. Fu, J.S. Ren and X. G. Qu, *Nucleic Acids Res.* 2008, **36**, 5695-5703

[2] C. Q. Zhao, J. Geng, L. Y. Feng, J. S. Ren and X. G. Qu, *Chem. Eur. J.* 2011, **17**, 8209-8215.

[3] R. J. White and K. W. Plaxco, *Anal. Chem.* 2010, **82**,73-76.

[4] K. Hsieh, R. J. White, B. S. Ferguson, K. W. Plaxco, Y. Xiao and H. T. Soh, *Angew. Chem., Int. Ed.* 2011, **50**, 11176-11180.

[5] M. A. Vorotyntsev, L. I. Daikhin and M. D. Levi, *J. Electroanal.Chem.* 1994, **364**, 37-49